Acta Crystallographica Section F
Structural Biology and Crystallization Communications
ISSN 1744-3091

Crystallization, X-ray diffraction analysis and SIRAS phasing of human α-L-iduronidase

Nobuo Maita,[a,b]* Hisaaki Taniguchi[b] and Hitoshi Sakuraba[c,d]

[a]Laboratory of X-ray Crystallography, Institute for Enzyme Research, University of Tokushima, 3-18-15, Kuramotocho, Tokushima 770-8503, Japan, [b]Division of Disease Proteomics, Institute for Enzyme Research, University of Tokushima, 3-18-15, Kuramotocho, Tokushima 770-8503, Japan, [c]Department of Analytical Biochemistry, Meiji Pharmaceutical University, 2-522-1, Noshio, Kiyose, Tokyo 204-8588, Japan, and [d]Department of Clinical Genetics, Meiji Pharmaceutical University, 2-522-1, Noshio, Kiyose, Tokyo 204-8588, Japan

Correspondence e-mail: nmaita@tokushima-u.ac.jp

Received 17 August 2012
Accepted 24 September 2012

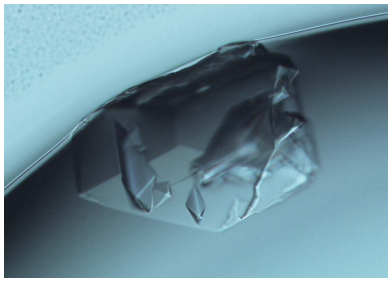

Human lysosomal α-L-iduronidase, whose deficiency causes mucopolysaccharidosis type I, was crystallized using sodium/potassium tartrate and polyethylene glycol 3350 as a precipitant. Using synchrotron radiation, a native data set was collected from a single crystal at 100 K to 2.3 Å resolution. The crystal belonged to space group $R3$ with unit-cell dimensions of $a = b = 259.22$, $c = 71.83$ Å. To obtain the phase information, mercury-derivative crystals were prepared and a single-wavelength anomalous dispersion (SAD) data set was collected at the Hg peak wavelength. Phase calculation with the single isomorphous replacement with anomalous scattering (SIRAS) method successfully yielded an interpretable electron-density map.

1. Introduction

Human α-L-iduronidase (hIDUA, EC: 3.2.1.76, UniProt ID: P35475) is a lysosomal enzyme that cleaves terminal α-iduronic acid residues from glycosaminoglycan, heparan sulfate and dermatan sulfate. The mature form of hIDUA has 626 amino acids (28–653) with molecular mass of 69 908 Da and includes six potential N-glycosylation sites. A deficiency of hIDUA causes one of the lysosomal storage diseases, mucopolysaccharidosis type I (MPS I). Patients with MPS I develop mental retardation, gross facial features, an enlarged and deformed skull, a small stature, corneal opacities, hepatosplenomegaly, valvular heart defects, thick skin, joint contractures and hernias. MPS I is classified into three subtypes based on its severity: Hurler (severe type), Hurler/Scheie (intermediate type) and Scheie (mild type) syndrome (Neufeld & Muenzer, 1989). Recently, enzyme replacement therapy for MPS I using recombinant hIDUA was introduced in clinical medicine (Kakkis *et al.*, 2001). Although many patients have been successfully treated with the recombinant enzyme, little improvement of brain and bone disorders is obtained. Thus, elucidation of the molecular mechanism of MPS I and a new therapeutic approach based on the new information are eagerly awaited.

Human α-L-iduronidase is classified into glycoside hydrolase family 39 (GH39) in the CAZy database (Henrissat & Davies, 1997). To date, the only experimentally determined structure of the GH39 family is that of bacterial β-xylosidase (XynB). Furthermore, a homology model of hIDUA constructed from *Thermoanaerobacterium saccharolyticum* XynB (PDB code 1px8; Yang *et al.*, 2004) has been reported. However, the sequence homology between hIDUA and *T. saccharolyticum* XynB is quite low (28.4% similarity) and thus the reliability of the model is not high. Furthermore, the amino-acid chain length of hIDUA is about 130 amino acids longer at the C-terminus than that of XynB (full length of 500 amino acids); therefore, the homology model is missing the C-terminal end of hIDUA (523–653), which includes eight point mutation sites reported in MPS I patients (Kang & Stevens, 2009).

So far, many mutations of the IDUA gene have been identified in MPS I patients (Scott *et al.*, 1995; Matte *et al.*, 2003; Yogalingam *et al.*, 2004). However, the details of the linkage between the mutations and MPS I symptoms remain unknown because of the lack of a precise three-dimensional structure of hIDUA. To elucidate the molecular pathology of MPS I and to develop new structure-based drugs for this disease, we crystallized recombinant hIDUA and collected X-ray

diffraction data to 2.3 Å resolution. Further, we prepared mercury-derivative crystals and successfully obtained a high-quality electron-density map through SIRAS (single isomorphous replacement with anomalous scattering) phasing.

2. Materials and methods

2.1. Protein preparation and crystallization

Recombinant hIDUA, expressed in Chinese hamster ovary (CHO) cells, was purchased from Genzyme Japan (marketed as Aldurazyme). The hIDUA was further purified on a Superdex 200 10/300 column (GE Healthcare) equilibrated with phosphate-buffered saline. The hIDUA-containing fractions, eluted at 14.5–15.5 ml, were pooled and concentrated with an Amicon Ultra (Millipore) with a pore size of 30 kDa, which resulted in an 8.0 mg ml^{-1} protein solution.

Initial crystallization screening was performed by hanging-drop vapour diffusion using Index and Crystal Screen 2 (Hampton Research), with drops consisting of 0.8 µl protein solution and 0.8 µl reservoir solution. The crystallization plates were kept at 288 K.

2.2. Preparation of heavy-atom derivatives

A heavy-atom derivative screening was carried out using Heavy Atom Screen Hg (Hampton Research). We prepared a number of 50 m*M* heavy-atom solutions, and then took 0.5 µl of each one and mixed it with 8 µl of a cryoprotectant solution, which resulted in a 3 m*M* heavy-atom solution. We transferred the crystal to a 2 µl drop of a heavy-atom solution and then the drop was vapour diffused against the reservoir solution for 12 h at 288 K. To obtain the high-quality data, we prepared an Hg derivative by co-crystallization as follows: 0.8 µl of the protein solution (4 mg ml^{-1}) was mixed with 0.8 µl of the heavy-atom solution [0.2 *M* K/Na tartrate, 20%(*w*/*v*) PEG 3350, 2 m*M* ethylmercuric phosphate and 5%(*v*/*v*) glycerol], followed by microseeding and vapour diffusion against 0.4 ml of the reservoir solution [0.2 *M* K/Na tartrate, 20%(*w*/*v*) PEG 3350 and 5%(*v*/*v*) glycerol].

2.3. X-ray data collection

Prior to data collection, crystals were picked up and dipped in a cryoprotectant solution [0.1 *M* MES–Na, pH 6.5, 18%(*w*/*v*) PEG 3350, 0.18 *M* Na/K tartrate and 15%(*v*/*v*) glycerol] for 10 s, flash-cooled with liquid nitrogen and then stored until data collection. The native data set was collected on beamline NW12A at the Photon Factory Advanced Ring (Tsukuba, Japan) using an ADSC Q210r detector with a crystal-to-detector distance of 246.2 mm and a wavelength of 1.0000 Å. We collected 180 frames with an oscillation angle of 1.2° and an exposure time of 3 s per frame. We kept the crystal at 100 K during data collection with a liquid nitrogen gas stream. The mercury-derivative crystal data set was collected on BL-17A at the Photon Factory (Tsukuba, Japan) using an ADSC Q315r detector with a wavelength of 1.0084 Å. The peak wavelength for the Hg L_{III} edge was determined by XAFS (X-ray absorption fine structure) measurement before the data collection. The crystal-to-detector distance was 448.5 mm, with an oscillation range of 1.2° per image, covering a total oscillation range of 360°. The diffraction data were processed with *HKL-2000* (Otwinowski & Minor, 1997), and merged and scaled against the native data.

Table 1
Statistics of diffraction data collection and SIRAS phasing.

Values in parentheses are for the highest-resolution shell. FOM = figure of merit

Crystal	Native	Hg peak
Data collection		
Space group	*R*3	*R*3
Unit-cell parameters (Å)	*a* = 259.22	*a* = 259.23
	b = 259.22	*b* = 259.23
	c = 71.83	*c* = 71.68
X-ray source	PF AR-NW12A	PF BL-17A
CCD detector	ADSC Q210r	ADSC Q315r
Wavelength (Å)	1.0000	1.0084
Resolution (Å)	40–2.3 (2.37–2.3)	30–3.1 (3.21–3.10)
No. of observed reflections	515171	375513
No. of unique reflections	78102	32378
Multiplicity	6.6 (4.4)	11.6 (11.5)
Completeness (%)	97.4 (80.6)	100 (100)
$\langle I\rangle/\langle\sigma(I)\rangle$	13.2 (3.0)	24.2 (12.3)
$R_{\rm merge}$† (%)	10.2 (46.8)	9.2 (22.8)
Crystal mosaicity (°)	0.377	0.482
SIRAS phasing		
Resolution (Å)		30–3.1
No. of heavy atoms in asymmetric unit		4
Phasing power (iso/ano)		0.632/0.590
⟨FOM⟩ (initial/after *SOLOMON*)		0.294/0.947
Asymmetric unit content		2 subunits

† $\sum_{hkl}\sum_i |I_i(hkl) - \langle I(hkl)\rangle| / \sum_{hkl}\sum_i I_i(hkl)$, where $I_i(hkl)$ is the intensity of the *i*th measurement of reflection *hkl* and $\langle I_i(hkl)\rangle$ is the average value of $I_i(hkl)$ for all *i* measurements.

2.4. SIRAS phasing

Phases were calculated by the SIRAS method including a heavy-atom search with *SHELXD* (Sheldrick, 2010), followed by phasing with *SHARP* (de La Fortelle & Bricogne, 1997) and density modification with *SOLOMON* (Abrahams & Leslie, 1996). All calculations were performed automatically using an *autoSHARP* package (Vonrhein *et al.*, 2007). The data-collection and phasing statistics are summarized in Table 1.

3. Results and discussion

3.1. Crystallization of hIDUA

We successfully obtained a wedge-shaped crystal using Index No. 86 [0.2 *M* K/Na tartrate and 20%(*w*/*v*) PEG 3350] as the precipitant in 2–3 d. Next, in order to improve the crystal, we performed additive

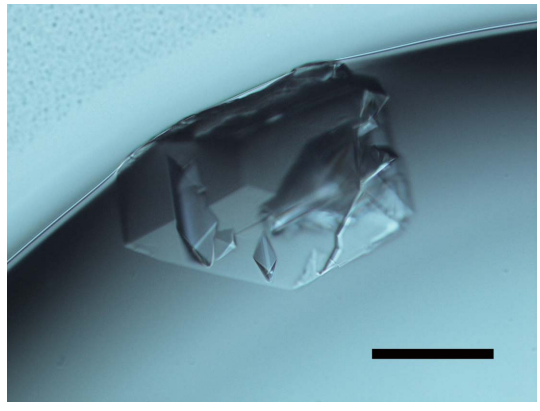

Figure 1
Crystal of hIDUA grown from 18%(*w*/*v*) PEG 3350, 0.18 *M* K/Na, tartrate, 3%(*w*/*v*) PEG MME 5000, 0.02 *M* ammonium sulfate and 0.01 *M* MES–Na, pH 6.5, at 288 K. Scale bar represents 0.1 mm.

screening by adding 10% of each solution in the Crystal Screen 2 kit. Finally, the best crystals were grown with the conditions consisting of 90% of Index No. 86 and 10% of Crystal Screen 2 No. 26 [18%(*w*/*v*) PEG 3350, 0.18 *M* K/Na tartrate, 3%(*w*/*v*) PEG MME 5000, 0.02 *M* ammonium sulfate and 0.01 *M* MES–Na, pH 6.5] (Fig. 1).

Prior to our study, Ruth *et al.* (2000) performed a crystallization study on recombinant human IDUA expressed in CHO cells; they could not produce good-quality crystals, only spherulites of semi-crystalline protein, when using PEG 8K and phosphate as precipitants. We suppose that the different results are partly due to the fact that Index was not marketed in 2000. In this study, we also observed round semi-crystalline particles with several PEG 3350 conditions such as Index Nos. 87 to 92.

3.2. X-ray data collection

The best crystal data set was collected at the Photon Factory on beamline AR-NW12A at a wavelength of 1.0000 Å and diffracted to a maximum resolution of 2.3 Å. Although the crystal had small clusters on its surface and weak diffraction spots from the clusters were observed (Fig. 2), the major crystal was large enough for us to process it with a good value of $R_{\rm merge}$ (10.2%), and no twinning was detected. The crystal belongs to space group *R*3 with cell parameters of $a = b = 259.22$, $c = 71.83$ Å.

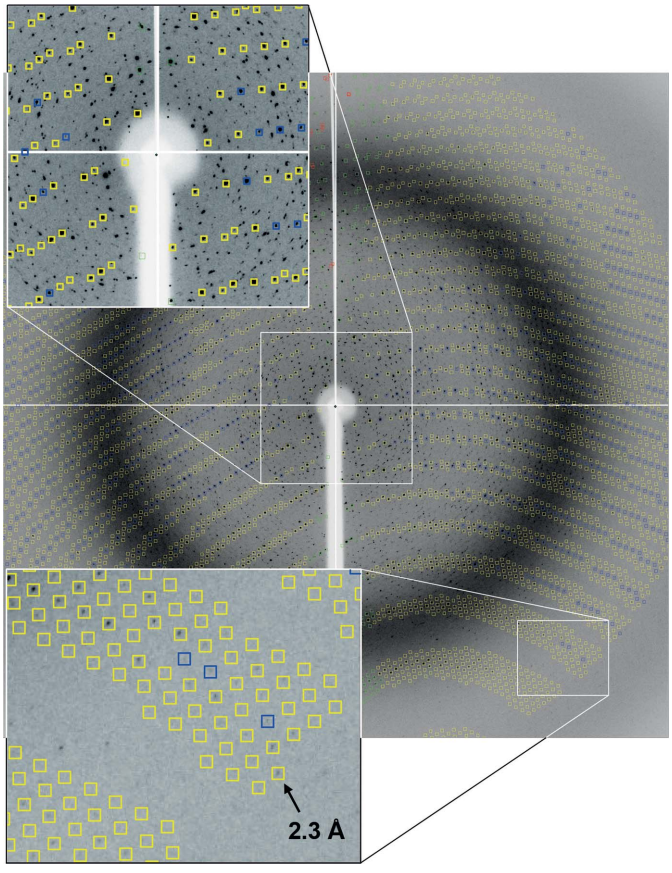

Figure 2
Representative X-ray diffraction image of native hIDUA collected with an oscillation angle of 1.2° and an exposure time of 3.0 s. Although many unassigned diffraction spots of small clusters were observed at lower resolution, the crystal diffracted up to 2.3 Å resolution.

3.3. Heavy-atom search and SIRAS phasing

Human IDUA belongs to the GH39 family in the CAZy classification (Henrissat & Davies, 1997). To date, only the crystal structure of bacterial β-xylosidase (XynB), which belongs to the same family, has been reported (Yang *et al.*, 2004; Czjzek *et al.*, 2005). Furthermore, Rempel *et al.* (2005) constructed a homology model of hIDUA (PDB code 1y24) based on the *T. saccharolyticum* XynB structure. First, we tried to solve the structure by molecular replacement with XynB or the homology model of IDUA, but no distinct solutions were obtained.

Next, we started heavy-atom-derivative screening. We tested Heavy Atom Screen Hg (Hampton Research), finding that ethylmercuric phosphate (EMP) bound to the protein and was suitable for phase determination. In order to collect high-quality heavy-atom data, we prepared Hg-derivative crystals by co-crystallization instead of soaking, because the crystals were so fragile that they tended to be damaged during the soaking operation.

We collected a full data set (to a resolution of 3.1 Å) for an Hg-derivative crystal with the peak wavelength for the Hg $L_{\rm III}$ edge ($\lambda = 1.0084$ Å) on PF BL-17A. The data were merged and scaled to the native data, followed by initial phasing calculation with the SIRAS method. We could observe distinct peaks in the Harker sections of both isomorphous and anomalous Patterson maps (Fig. 3), and a subsequent heavy-atom search indicated four mercury atoms

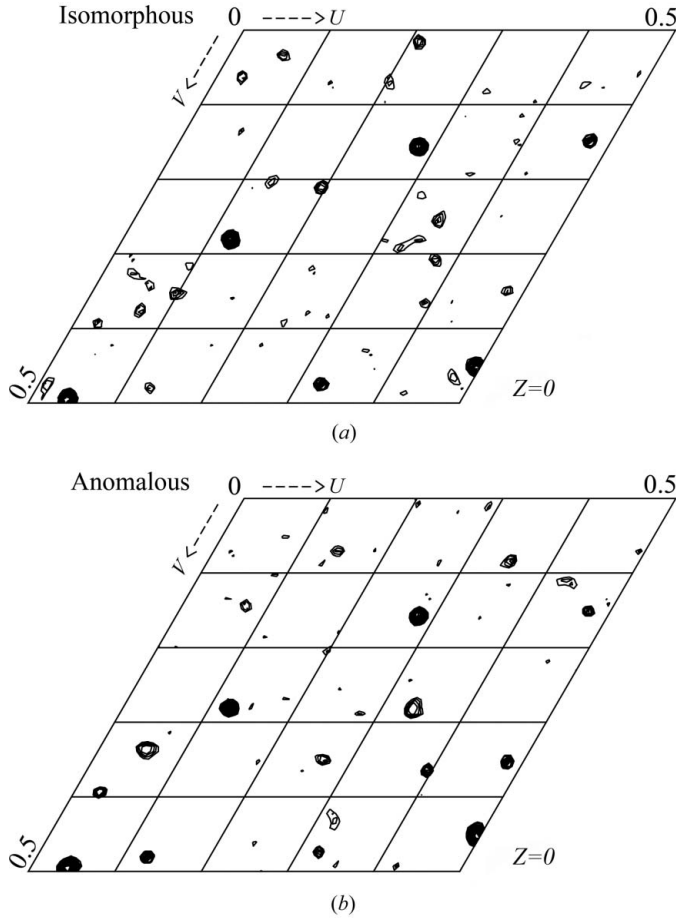

Figure 3
The Harker sections ($Z = 0$) of (*a*) isomorphous and (*b*) anomalous difference Patterson maps (contoured at 1.75σ), with the highest peak σ of 10.8σ and 12.1σ, respectively. The maps were calculated within the resolution range of 25–5 Å.

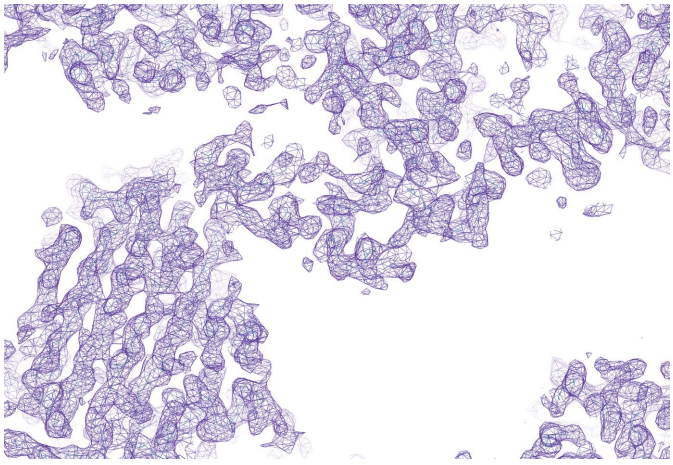

Figure 4
Experimental electron-density map (contoured at 1σ) calculated from the SIRAS phase after solvent flattening. The figure was prepared with *Coot* (Emsley *et al.*, 2010).

per asymmetric unit. After the density modification, we had a high-quality interpretable map (Fig. 4). According to the optimal solvent content estimation by *autoSHARP* (Vonrhein *et al.*, 2007), there are two subunits per asymmetric unit, with a solvent content of 55% and a V_M value of 3.31 Å^3 Da^{-1} (Matthews, 1968). The refinement of the hIDUA structure is now underway. The details of the structure and a catalytic description of hIDUA will be published elsewhere.

We thank the beamline staff at the Photon Factory for supporting the data collection under proposal Nos. 2009 G074 and 2011 G135. This work was partly supported by Grants-in-Aid for Young Scientists (grant No. 20770085) and Scientific Research (grant No. 23570139) from the Ministry of Education, Culture, Sports, Science and Technology, Japan, to NM.

References

Abrahams, J. P. & Leslie, A. G. W. (1996). *Acta Cryst.* D**52**, 30–42.
Czjzek, M., Ben David, A., Bravman, T., Shoham, G., Henrissat, B. & Shoham, Y. (2005). *J. Mol. Biol.* **353**, 838–846.
Emsley, P., Lohkamp, B., Scott, W. G. & Cowtan, K. (2010). *Acta Cryst.* D**66**, 486–501.
Henrissat, B. & Davies, G. (1997). *Curr. Opin. Struct. Biol.* **7**, 637–644.
Kakkis, E. D., Muenzer, J., Tiller, G. E., Waber, L., Belmont, J., Passage, M., Izykowski, B., Phillips, J., Doroshow, R., Walot, I., Hoft, R. & Neufeld, E. F. (2001). *N. Engl. J. Med.* **344**, 182–188.
Kang, T. S. & Stevens, R. C. (2009). *Hum. Mutat.* **30**, 1591–1610.
La Fortelle, E. de & Bricogne, G. (1997). *Methods Enzymol.* **276**, 472–494.
Matte, U., Yogalingam, G., Brooks, D., Leistner, S., Schwartz, I., Lima, L., Norato, D. Y., Brum, J. M., Beesley, C., Winchester, B., Giugliani, R. & Hopwood, J. J. (2003). *Mol. Genet. Metab.* **78**, 37–43.
Matthews, B. W. (1968). *J. Mol. Biol.* **33**, 491–497.
Neufeld, E. F. & Muenzer, J. (1989). *The Metabolic Basis of Inherited Disease*, edited by C. R. Scriver, M. C. Beaudet, W. S. Sly & D. Valle, pp. 1565–1587. New York: McGraw-Hill.
Otwinowski, Z. & Minor, W. (1997). *Methods Enzymol.* **276**, 307–326.
Rempel, B. P., Clarke, L. A. & Withers, S. G. (2005). *Mol. Genet. Metab.* **85**, 28–37.
Ruth, L., Eisenberg, D. & Neufeld, E. F. (2000). *Acta Cryst.* D**56**, 524–528.
Scott, H. S., Bunge, S., Gal, A., Clarke, L. A., Morris, C. P. & Hopwood, J. J. (1995). *Hum. Mutat.* **6**, 288–302.
Sheldrick, G. M. (2010). *Acta Cryst.* D**66**, 479–485.
Vonrhein, C., Blanc, E., Roversi, P. & Bricogne, G. (2007). *Methods Mol. Biol.* **364**, 215–230.
Yang, J. K., Yoon, H. J., Ahn, H. J., Lee, B. I., Pedelacq, J. D., Liong, E. C., Berendzen, J., Laivenieks, M., Vieille, C., Zeikus, G. J., Vocadlo, D. J., Withers, S. G. & Suh, S. W. (2004). *J. Mol. Biol.* **335**, 155–165.
Yogalingam, G., Guo, X. H., Muller, V. J., Brooks, D. A., Clements, P. R., Kakkis, E. D. & Hopwood, J. J. (2004). *Hum. Mutat.* **24**, 199–207.